The Plant Cell, Vol. 26: 485–496, January 2014, www.plantcell.org

An E4 Ligase Facilitates Polyubiquitination of Plant Immune Receptor Resistance Proteins in *Arabidopsis*[W]

Yan Huang,[a,b] Sean Minaker,[a] Charlotte Roth,[c] Shuai Huang,[a,b] Philip Hieter,[a] Volker Lipka,[c] Marcel Wiermer,[c] and Xin Li[a,b,1]

[a] Michael Smith Laboratories, University of British Columbia, Vancouver, British Columbia V6T 1Z4, Canada
[b] Department of Botany, University of British Columbia, Vancouver, British Columbia V6T 1Z4, Canada
[c] Department of Plant Cell Biology, Albrecht-von-Haller-Institute for Plant Sciences, Georg-August-University Goettingen, 37077 Goettingen, Germany

Proteins with nucleotide binding and leucine-rich repeat domains (NLRs) serve as immune receptors in animals and plants that recognize pathogens and activate downstream defense responses. As high accumulation of NLRs can result in unwarranted autoimmune responses, their cellular concentrations must be tightly regulated. However, the molecular mechanisms of this process are poorly detailed. The F-box protein Constitutive expressor of *PR* genes 1 (CPR1) was previously identified as a component of a Skp1, Cullin1, F-box protein E3 complex that targets NLRs, including Suppressor of NPR1, Constitutive 1 (SNC1) and Resistance to *Pseudomonas syringae* 2 (RPS2), for ubiquitination and further protein degradation. From a forward genetic screen, we identified Mutant, *snc1*-enhancing 3 (MUSE3), an E4 ubiquitin ligase involved in polyubiquitination of its protein targets. Knocking out *MUSE3* in *Arabidopsis thaliana* results in increased levels of NLRs, including SNC1 and RPS2, whereas overexpressing *MUSE3* together with *CPR1* enhances polyubiquitination and protein degradation of these immune receptors. This report on the functional role of an E4 ligase in plants provides insight into the scarcely understood NLR degradation pathway.

INTRODUCTION

Plants have evolved complex immune systems to fight invading microbial pathogens that threaten normal growth and development. Resistance (R) protein–mediated defense is an effective mechanism that senses the molecular activities of secreted pathogen effector molecules, such as AvrB and AvrRpt2, through either direct or indirect recognition (Staskawicz et al., 1995; Bent and Mackey, 2007). Most R proteins share homology with animal nucleotide binding oligomerization domain receptors, with common structural features including a central nucleotide binding domain and C-terminal Leu-rich repeats (Maekawa et al., 2011). Plant nucleotide binding and leucine-rich repeat (NLR) R proteins can be further divided into two subclasses based on their N-terminal coiled-coil or Toll/Interleukin1 receptor domains (Aarts et al., 1998). Upon effector recognition, NLR R proteins activate diverse downstream responses that usually culminate in a hypersensitive response to effectively restrict further pathogen spread (Jones and Dangl, 2006). NLR R protein levels have to be tightly regulated to enable appropriate defense output and to avoid autoimmunity caused by R protein overaccumulation.

Autoimmune mutants, such as *suppressor of npr1-1, constitutive 1* (*snc1*) and *suppressor of salicylic acid insensitivity of npr1-5, 4* (*ssi4*), in which NLR R protein activity or stability is enhanced, exhibit constitutive defense phenotypes, including elevated defense marker gene expression, accumulation of the defense hormone salicylic acid, and enhanced pathogen resistance, all of which contribute to reduced plant growth (Li et al., 2001; Shirano et al., 2002). In order to balance plant immunity with proper growth and development, NLR R protein activity and turnover need to be tightly controlled (Shirasu, 2009). However, the molecular mechanism by which NLR R protein levels are controlled is unclear. There is growing evidence suggesting that ubiquitination plays an important role in NLR R protein–mediated immunity (Liu et al., 2002; Zeng et al., 2004; Trujillo and Shirasu, 2010; Cheng and Li, 2012). Recent research revealed that the F-box protein Constitutive expressor of PR genes 1 (CPR1), a subunit of the E3 ubiquitin (Ub) ligase complex SKP1-CULLIN1-F-box (SCF), targets R proteins, including SNC1 and Resistance to *Pseudomonas syringae* 2 (RPS2), for degradation to prevent R protein overaccumulation and resultant autoimmunity (Cheng et al., 2011; Gou et al., 2012). Thus, Ub/proteasome-mediated degradation may function as a crucial mechanism for regulating the turnover of plant R proteins.

In eukaryotes, degradation of selective target proteins such as transcription factors, cell cycle regulators, signal transducers, and misfolded proteins often occurs through the Ub/proteasome pathway (Hershko and Ciechanover, 1998). Ubiquitination is achieved by a series of well-characterized reactions catalyzed by enzymes, including Ub-activating enzyme E1, Ub-conjugating enzyme E2, and Ub ligase E3, which add Ub moieties to their substrates, typically marking them for subsequent degradation (Hochstrasser, 1996; Pickart, 2001). In vitro ubiquitination assays have demonstrated that the combined activities of E1, E2, and E3 enzymes are necessary and sufficient for the recognition and ubiquitination of many target substrates. Although polyubiquitinated

[1] Address correspondence to xinli@msl.ubc.ca.
The author responsible for distribution of materials integral to the findings presented in this article in accordance with the policy described in the Instructions for Authors (www.plantcell.org) is: Xin Li (xinli@msl.ubc.ca).
[W] Online version contains Web-only data.
www.plantcell.org/cgi/doi/10.1105/tpc.113.119057

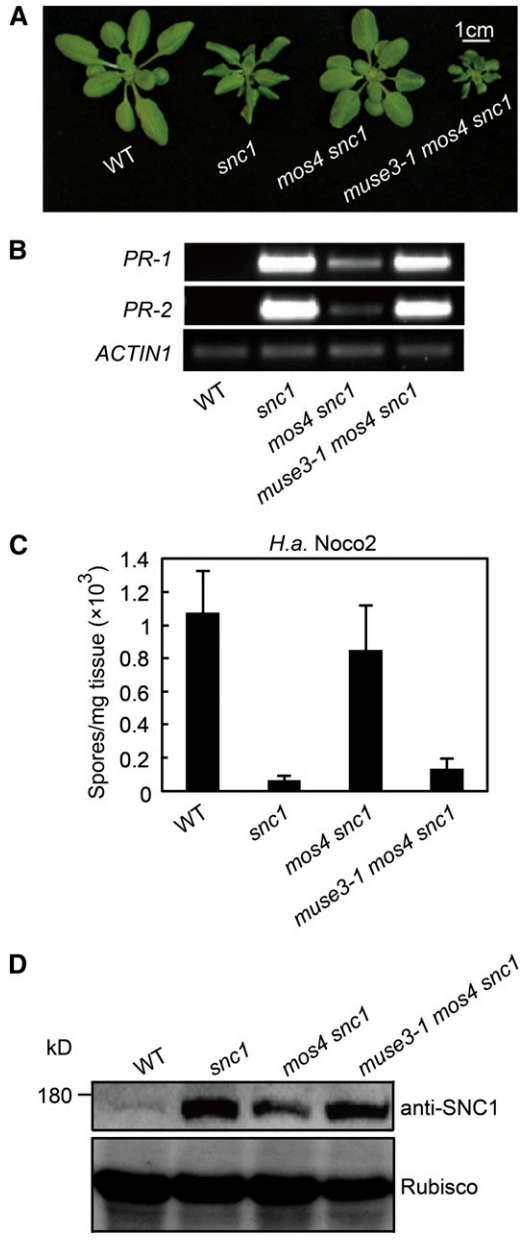

Figure 1. Characterization of the *muse3-1 mos4 snc1* Triple Mutant.

(A) Morphology of 3-week-old soil-grown plants of the wide type, *snc1*, *mos4 snc1*, and *muse3-1 mos4 snc1*. Bar = 1 cm.

(B) Total RNA was extracted from 2-week-old plants grown on half-strength MS medium and reverse transcribed to cDNA. *PR-1*, *PR-2*, and *ACTIN1* were amplified by 28 cycles of PCR using equal amounts of total cDNA, and the products were analyzed by agarose gel electrophoresis.

(C) Quantification of *H. arabidopsidis* (*H.a.*) Noco2 sporulation on the wild type, *snc1*, *mos4 snc1*, and *muse3-1 mos4 snc1* plants. Two-week-old seedlings were inoculated with *H. a.* Noco2 at a concentration of 10^5 spores per 1 mL of water. The spores were quantified 7 d after inoculation. Data are mean values of four replicates ± SD.

(D) SNC1 protein levels in the indicated genotypes. Total protein was extracted from leaves of 4-week-old soil-grown plants. SNC1 protein was examined by immunoblot analysis with an anti-SNC1 antibody, which was generated against an SNC1-specific peptide in rabbit (Li et al., 2010). Rubisco levels from Ponceau S staining served as an internal loading control.

proteins are the preferred substrates of the 26S proteasome, only a few Ub moieties can be efficiently added to the substrate by E1, E2, and E3 enzymes alone. Efficient polyubiquitination beyond two or three Ubs often relies on E4 ligase activity (Koegl et al., 1999). In yeast, Ub-conjugating E4 factor Ubiquitin Fusion Degradation Protein2 (UFD2) facilitates polyubiquitin chain assembly in conjunction with E1, E2, and E3s. The current model for E4 function in animals and yeast suggests that it may form E3-E4 or E4-substrate complexes to coordinate the transfer of Ub from E2 to the substrate or sequentially add Ub to the substrate after E3 initially ubiquitinates the target (Koegl et al., 1999; Hoppe et al., 2004).

Yeast E4 UFD2 is an evolutionarily conserved protein with a C-terminal U-box domain. A number of E4 orthologs have been functionally studied so far: the yeast UFD2, the human or mouse Ubiquitin factor E4A/E4B (UBE4A/UBE4B), the *Caenorhabditis elegans* UFD2, and NOSA from *Dictyostelium* (Johnson et al., 1995; Pukatzki et al., 1998; Koegl et al., 1999; Hoppe et al., 2004; Matsumoto et al., 2004). Here, we report the isolation, characterization, positional cloning, and functional analysis of *Arabidopsis thaliana MUSE3* (for Mutant, *snc1*-enhancing 3), which encodes a Ub-conjugating E4 factor. Our study reveals that MUSE3 functions as an E4 factor and works downstream of the E3 ligase SCF^{CPR1} to facilitate the polyubiquitination and degradation of R proteins, including SNC1 and RPS2.

RESULTS

The *muse3-1* Mutation Enhances *snc1*-Mediated Autoimmunity in the *mos4 snc1* Background

In *Arabidopsis*, the dominant mutant *snc1* exhibits constitutive activation of plant defense responses, including elevated defense marker gene expression and enhanced resistance against both bacterial and oomycete pathogens (Li et al., 2001; Zhang et al., 2003). The mutant *modifier of snc1, 4* (*mos4-1*) allele, which was originally identified as a genetic suppressor of *snc1*, reverts *snc1* to wild-type-like phenotypes in the *snc1* background (Palma et al., 2007). The triple mutant *muse3-1 mos4 snc1* was isolated from the recently described *muse* forward genetic screen in the *mos4-1 snc1* background that was designed to isolate negative regulators of R protein–mediated immunity (Huang et al., 2013). When backcrossed to *mos4 snc1*, wild-type-like morphology was observed in all F1 progeny, suggesting that the *muse3-1* mutation is recessive. As shown in Figure 1A, this triple mutant reverts to an *snc1*-like morphology despite the presence of the *mos4* allele, exhibiting more severe dwarfism than *snc1*.

To confirm that other defense-related phenotypes are enhanced in the *muse3-1 mos4 snc1* mutant, the expression levels of defense marker *Pathogenesis Related* (*PR*) genes *PR-1* and *PR-2* were examined by RT-PCR. As shown in Figure 1B,

expression of both *PR-1* and *PR-2* was increased to *snc1*-like levels in the triple mutant. Consistently, the *snc1*-like enhanced resistance against the virulent pathogen *Hyaloperonospora arabidopsidis* Noco2 was restored in the *muse3-1 mos4 snc1* seedlings (Figure 1C). As *snc1* exhibits higher SNC1 protein accumulation compared with the wild type (Cheng et al., 2011), which can be partially suppressed by *mos4*, the SNC1 level was also examined in the triple mutant. As shown in Figure 1D, the SNC1 protein level in the triple mutant is similar to that in *snc1*. Taken together, *muse3-1* enhances all *snc1*-associated defense phenotypes in the *mos4 snc1* background.

Positional Cloning of *muse3-1*

To identify *muse3-1*, a positional cloning approach was utilized. Triple mutant *muse3-1 mos4 snc1* (in the *Arabidopsis* ecotype Columbia background) was crossed with *Arabidopsis* ecotype Landsberg *erecta*. F1 plants were allowed to self-fertilize to generate a segregating F2 population. Using 24 F2 plants with *snc1*-enhancing morphology as a crude mapping population, the *muse3-1* mutation was mapped to the top arm of chromosome 5 through linkage analysis. The mutation was further flanked by markers T31P16 and MPI7 using an additional 96 *snc1*-enhancing F2 plants (Figure 2A). To confirm the initial mapping and further localize the mutation region, a larger fine-mapping population was generated using progeny from several F2 lines that are heterozygous for the *muse3-1* mutation but homozygous at both *SNC1* (*snc1*) and *MOS4* (*mos4*), aiming to avoid interference from those two loci. With 549 F3 plants from the fine-mapping population, 69 recombinants were found between T31P16 and MPI7. As shown in Figure 2A, the *muse3-1* mutation was eventually found to lie between markers T9L3 and MQK4 and was located on BAC clone T20K14.

To identify potential molecular lesions in *muse3-1*, Illumina whole-genome sequencing was performed on nuclear DNA isolated from *muse3-1 mos4 snc1* plants. After comparison between mutant and the *Arabidopsis* wild-type reference genome sequences, several candidate genes with mutations were identified. Some of the mutations could be excluded as candidates after detailed sequence analysis, because they were either false positive or silent mutations that did not cause amino acid changes. Direct Sanger sequencing confirmed the most likely candidate gene mutation using genomic DNA from *muse3-1 mos4 snc1*. A C-to-T transition occurred in *At5g15400* in the 10th exon (Figures 2B and 2C), changing Gln-789 to an early stop codon and truncating the predicted U-box domain of the protein (Figure 2D).

BLAST analysis revealed that *MUSE3* is a single-copy gene encoding a putative Ub-conjugating E4 factor with a conserved central Ub-elongating factor core domain (also called the UFD2p core domain) and a C-terminal U-box domain (Figure 2D). Phylogenetic analysis of MUSE3 and its homologs showed that MUSE3 is a highly conserved protein in all sequenced eukaryotes (Supplemental Figure 1). The best studied MUSE3 homolog is the yeast E4 Ub ligase UFD2, which promotes Ub chain elongation of various target substrates (Hoppe, 2005). MUSE3 shares 35 and 30% amino acid similarity with UFD2 and UBE4, respectively. Protein alignment of the predicted UFD2p core domains and the U-boxes between MUSE3 and UFD2 further confirmed that these domains share high sequence homology and are highly conserved (Supplemental Figure 2).

The SAIL_713_A12 T-DNA insertion allele of *muse3*, renamed *muse3-2*, was obtained from the ABRC. *muse3-2* carries a T-DNA insertion in the 11th exon of *At5g15400* (Figure 2B). To test whether *muse3-2* is allelic to *muse3-1*, a homozygous *muse3-2* plant was crossed with homozygous *muse3-1 mos4 snc1*. In the F1 generation, all the plants exhibit a similar dwarfism to *muse3-1 mos4 snc1* (Figure 2E), indicating that *muse3-2* fails to complement *muse3-1* and that *muse3-2* is allelic to *muse3-1*.

MUSE3 Encodes a Putative Ub-Conjugating E4 Factor That Localizes to Both Nucleus and Cytoplasm

To confirm that the mutation found in *At5g15400* is responsible for the *muse3* mutant phenotypes and to better understand the function of MUSE3, full-length genomic clones of *At5g15400* under the control of its native promoter with or without a C-terminal *Green Fluorescent Protein* (*GFP*) gene were transformed into *muse3-1 mos4 snc1* plants. As shown in Figures 3A and 3B and Supplemental Figures 3A and 3B, both transgenes are able to complement the morphological and enhanced resistance phenotypes of *muse3-1 mos4 snc1*. Combined with the aforementioned allelism test, all these data suggest that *MUSE3* is *At5g15400* and that MUSE3-GFP is functional and should localize to its proper subcellular compartment(s).

To assess the subcellular localization of MUSE3, *MUSE3-GFP* transgenic plants were examined by two independent approaches: confocal fluorescence microscopy and subcellular fractionation followed by immunoblot analysis. MUSE3-GFP fluorescence was observed in both nuclei and cytoplasm of leaf epidermal and root cells (Figure 3C). Subcellular fractionation confirmed that MUSE3-GFP is indeed present in both the nuclei-depleted and nuclei-enriched fractions (Supplemental Figure 4). Thus, MUSE3 seems ubiquitous, having both nuclear and cytoplasmic localizations.

Arabidopsis MUSE3 Complements the Yeast *ufd2*Δ Mutant Phenotypes

Previously, the yeast knockout strain *ufd2*Δ was shown to exhibit growth defects including sensitivity to ethanol or hydroxyurea at 37°C (Koegl et al., 1999). Since UFD2 is a close homolog of MUSE3, we tested whether MUSE3 is orthologous to UFD2 using a yeast complementation experiment. As shown in Figure 4, the *ufd2*Δ mutant strain exhibits no growth defect on SD-Leu plates. However, compared with the wild-type strain, *ufd2*Δ cells did not grow well and exhibited obvious sensitivity to either 10% ethanol or 100 mM hydroxyurea. By contrast, *ufd2*Δ cells expressing *MUSE3* grew much better on plates containing 10% ethanol than did the *ufd2*Δ strain, although not as well as wild-type cells. Furthermore, *ufd2*Δ strains expressing *MUSE3* grew as well as the wild type on plates containing 100 mM hydroxyurea. These data demonstrate that *Arabidopsis MUSE3* is able to complement the *ufd2*Δ knockout phenotypes, suggesting that MUSE3 is a functional ortholog of the yeast UFD2 E4 ligase that is involved in Ub chain elongation.

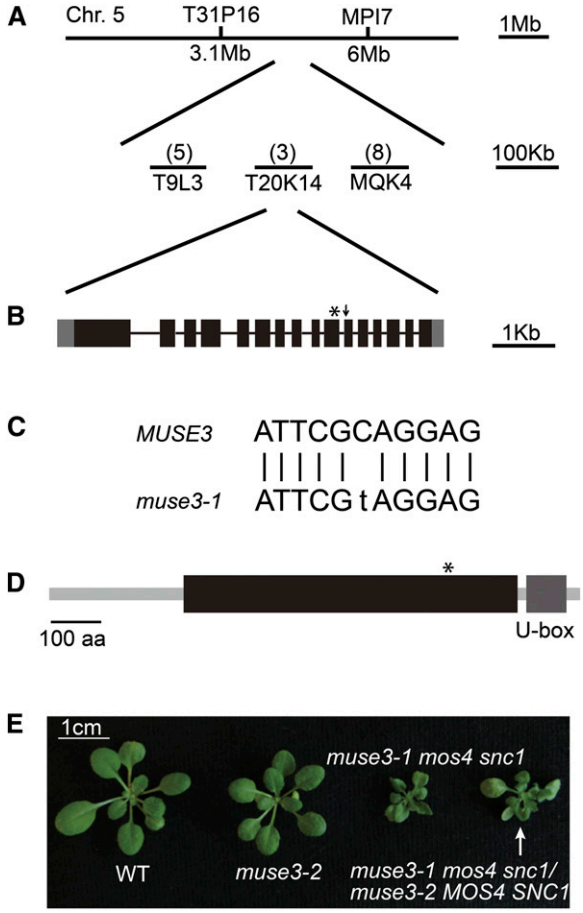

Figure 2. Positional Cloning of *muse3-1*.

(A) Map position of *muse3-1* on chromosome 5. BAC clones and numbers of recombinants from the mapping population (in parentheses) are indicated.
(B) Gene structure of *MUSE3* (*At5g15400*). There is only one known splice form of *MUSE3*. Boxes indicate exons and lines indicate introns. Gray regions represent untranslated regions, and black regions represent coding regions. The asterisk indicates the site of the C-to-T mutation in *muse3-1*. The arrow indicates the position of the T-DNA insertion site in *muse3-2*.
(C) Genomic DNA sequence comparison between *MUSE3* and *muse3-1*. In *muse3-1*, a C-to-T point mutation occurs in the 10th exon and is indicated as a lowercase letter.
(D) The predicted protein domains of MUSE3. One UFD2p core domain is indicated as a long black rectangle. The short rectangle represents the U-box domain. The asterisk indicates where the protein truncation occurs due to the mutation in *muse3-1*. Bar = 100 amino acids.
(E) Morphology of 3-week-old plants of the wild type, *muse3-2*, and *muse3-1 mos4 snc1* and F1 of *muse3-2* crossed with *muse3-1 mos4 snc1*. The genotypes of the F1 plants were confirmed by PCR using mutation-specific primers. Because *snc1* morphology is semidominant and *mos4* is recessive, severely dwarfed F1 progeny suggest failed complementation between *muse3-1* and *muse3-2*, both of which are recessive. Bar = 1 cm.

muse3 Mutants Exhibit Enhanced Disease Resistance Phenotypes

Our study of the *muse3-1 mos4 snc1* triple mutant indicates that MUSE3 functions as a negative regulator of *snc1*-mediated immunity. To determine its general role in plant immunity, we generated the *muse3-1* single mutant by crossing *muse3-1 mos4 snc1* with wild-type plants, followed by allele-specific genotyping in the F2 generation. We also utilized the *muse3-2* allele for single mutant analyses. As shown in Figure 5A, both *muse3-1* and *muse3-2* plants resemble wild-type plants, having a slightly smaller size as quantified by fresh weight analysis of

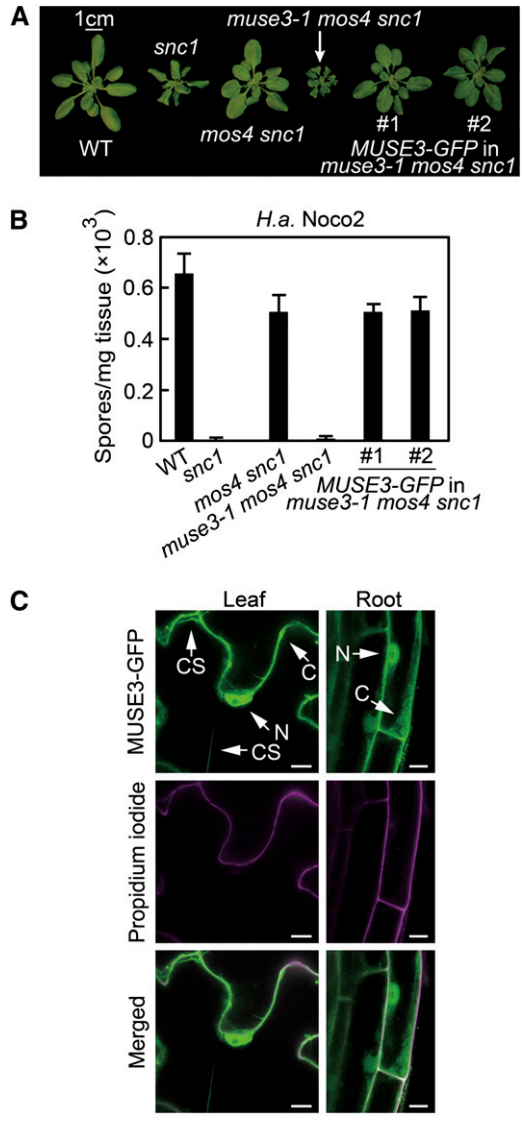

Figure 3. *MUSE3-GFP* Complements the Molecular Lesion in *muse3-1* and Localizes to Both Nuclei and Cytoplasm.

(A) Morphology of the wild type, *snc1*, *mos4 snc1*, *muse3-1 mos4 snc1*, and two representative transgenic lines expressing *MUSE3-GFP* under the control of its native promoter in the *muse3-1 mos4 snc1* triple mutant background. Bar = 1 cm.
(B) Quantification of *H. arabidopsidis* (*H.a.*) Noco2 sporulation for the indicated genotypes. Data are mean values of four replicates ± SD.
(C) Confocal images of MUSE3-GFP fluorescence in leaf epidermis and root cells of plate-grown *muse3-1 mos4 snc1* transgenic plants expressing *MUSE3-GFP*. Cell walls were stained with propidium iodide to visualize the cell outlines. C, cytoplasm; CS, cytoplasmic strands; N, nucleus. Bars = 10 μm.

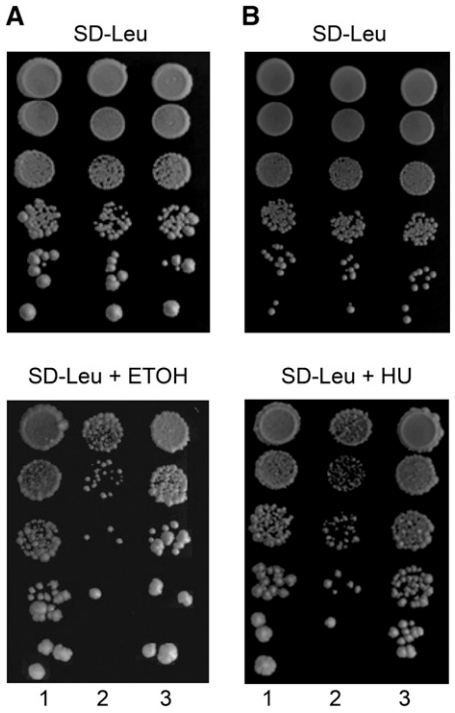

Figure 4. *MUSE3* Complements the *S. cerevisiae ufd2*Δ Knockout Phenotypes.

The following yeast strains were grown to early log phase and serially diluted and spotted on the indicated media: lane 1, wild-type yeast strain expressing p425-GPD empty vector; lane 2, yeast *ufd2*Δ knockout strain expressing p425-GPD empty vector; lane 3, *ufd2*Δ knockout strain expressing p425-GPD-*MUSE3*. Plates containing the following media were incubated at 37°C for several days as indicated: synthetic defined (SD)-Leu + 10% ethanol (ETOH), incubated for 6 d **(A)**; and SD-Leu + 100 mM hydroxyurea (HU), incubated for 3 d **(B)**. The SD-Leu plates shown in the top panels were used as equal inoculum controls.

aerial tissues (Figure 5B). The relative expression levels of *PR-1* and *PR-2* were increased in both mutant alleles (Figure 5C). To determine whether *muse3* also altered resistance against virulent pathogens, *muse3-1*, *muse3-2*, and wild-type control plants were challenged with the virulent oomycete *H. arabidopsidis* Noco2 or the bacterial pathogen *Pseudomonas syringae* pv *maculicola* ES4326. As shown in Figures 5D and 5E, resistance against both pathogens was enhanced by both *muse3* mutations. Because SNC1 accumulates in the *muse3-1 mos4 snc1* triple mutant, the SNC1 level was also examined in *muse3* single mutants. As shown in Figure 5F, both *muse3-1* and *muse3-2* exhibited higher SNC1 protein levels, although wild-type-like *SNC1* transcription levels were detected (Figure 5C). These data indicate that mutations in *MUSE3* cause enhanced disease resistance and stabilize SNC1.

Constitutive Defense Responses in *muse3-2* Are Partially Suppressed by Knocking Out *SNC1*

To test whether the enhanced resistance responses in the *muse3* mutants are due to increased accumulation of SNC1 protein, we introduced *snc1-r1*, a loss-of-function deletion allele of *SNC1* (Zhang et al., 2003), into *muse3-2*. Analysis of *PR* gene expression showed that constitutive expression of both *PR-1* and *PR-2* was only partially reduced in *muse3-2 snc1-r1* (Figure 6A). In addition, enhanced resistance against the virulent pathogen *H. arabidopsidis* Noco2 in *muse3-2* was partially suppressed by the *snc1-r1* mutation (Figure 6B). However, knocking out *SNC1* did not significantly affect the *muse3-2*–associated resistance against *Pseudomonas* ES4326 (Figure 6C). These data suggest that the overaccumulation of SNC1 in *muse3-2* contributes only partially to the enhanced resistance phenotypes of *muse3*, indicating that MUSE3 may target additional NLRs other than SNC1 for degradation.

To test whether MUSE3 affects the stability of the coiled-coil type NLR RPS2, we crossed the previously reported *RPS2-HA* transgene into the *muse3-2* background (Axtell and Staskawicz, 2003). As shown in Figure 6D, RPS2-HA accumulates more in *muse3-2*, indicating that MUSE3 also contributes to the turnover of RPS2. Without MUSE3, RPS2 becomes more stable.

MUSE3 Facilitates the Degradation of SNC1 and RPS2 Mediated by CPR1

The phenotypic analysis of *muse3* mutants suggests that MUSE3 may negatively regulate the stability of SNC1 and RPS2. As the F-box protein CPR1, a component of the SCF E3 complex, has been shown to target SNC1 and RPS2 for degradation (Cheng et al., 2011), we hypothesized that MUSE3 may function together with CPR1 to regulate SNC1 and RPS2 degradation through the Ub/proteasome pathway. To test this hypothesis, we employed a transient expression system in *Nicotiana benthamiana* by coexpressing *SNC1-FLAG* or *RPS2-FLAG* with either *CPR1-FLAG* or *MUSE3-HA* alone or *CPR1-FLAG* and *MUSE3-HA* together to reveal their biochemical relationships (Gou et al., 2012). As shown in Figures 7A and 7B, when coexpressed with *CPR1*, SNC1 and RPS2 exhibit decreased accumulation compared with expressing *SNC1* or *RPS2* alone, which is consistent with CPR1 targeting SNC1 and RPS2 for degradation (Cheng et al., 2011; Gou et al., 2012). When coexpressed with *MUSE3*, both SNC1 and RPS2 expression levels were unaffected, indicating that, unlike CPR1, MUSE3 does not function as an E3 by itself that directly targets these substrates for degradation. However, when coexpressed with both *CPR1* and *MUSE3*, the protein levels of SNC1 and RPS2 were much lower than when coexpressed with *CPR1* alone, demonstrating that MUSE3 facilitates the degradation of SNC1 and RPS2 mediated by the E3 SCF^{CPR1}. A similar trend in SNC1 levels was observed in *snc1* overexpressing both *CPR1* and *MUSE3-GFP* in *Arabidopsis*. Overexpression of CPR1 reduces the level of SNC1 and suppresses *snc1*-mediated dwarfism (Figures 7C and 7D), whereas overexpression of MUSE3-GFP alone did not alter either the SNC1 level or the morphological phenotypes of *snc1*. However, the SNC1 level was further reduced when MUSE3-GFP was expressed together with CPR1 (Figures 7C and 7D). Interestingly, we sometimes were able to detect polyubiquitinated RPS2 when it was coexpressed with both CPR1 and MUSE3 in *N. benthamiana*, supporting the role of MUSE3 as an E4 in polyubiquitination (Supplemental Figure 5). However, we never

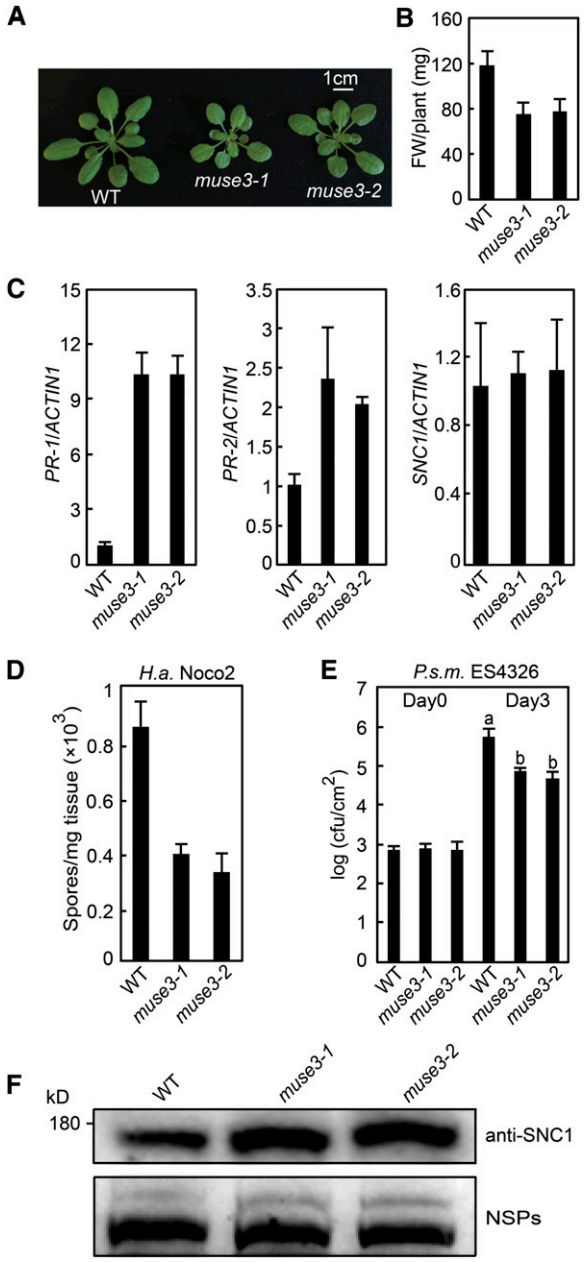

Figure 5. Characterization of Two *muse3* Single Mutant Alleles.

(A) Morphology of 4-week-old soil-grown plants of the wild type, *muse3-1*, and *muse3-2*. Bar = 1 cm.

(B) Aerial fresh weight (FW) of 3-week-old plants of the indicated genotypes. Bars represent means of 12 replicates ± SD. The experiments were repeated three times with similar results.

(C) Relative expression of *PR-1*, *PR-2*, and *SNC1* in the wild type, *muse3-1*, and *muse3-2* as determined by real-time RT-PCR. Total RNA was extracted from 2-week-old plants grown on half-strength MS plates and reverse transcribed to cDNA. The *PR-1*, *PR-2*, and *SNC1* expression levels were normalized using *ACTIN1*. Bars represent means of three replicates ± SD. The experiment was repeated three times with similar results.

(D) Quantification of *H. arabidopsidis* (*H.a.*) Noco2 sporulation on wild-type, *muse3-1*, and *muse3-2* seedlings. Data are mean values of four replicates ± SD.

observed polyubiquitinated forms of SNC1, even from proteasome inhibitor MG132-pretreated leaf samples (Supplemental Figure 6), possibly due to transience or instability of the polyubiquitinated forms of the substrate protein.

The genetic and biochemical associations between MUSE3 and SNC1, RPS2, and CPR1 prompted us to test whether MUSE3 interacts with SNC1, RPS2, or CPR1 in planta. Coimmunoprecipitation (Co-IP) using coexpressed MUSE3-HA with either SNC1-FLAG, RPS2-FLAG, or CPR1-FLAG fusion protein in *N. benthamiana* with anti-FLAG agarose beads revealed that MUSE3-HA coimmunoprecipitated only with SNC1, but not with RPS2 or CPR1, in the elution fractions (Figures 8A to 8C). These results were confirmed by reciprocal Co-IP experiments using anti-HA agarose beads (Supplemental Figures 7A to 7C). Taken together, MUSE3 seems to function downstream of CPR1 to facilitate the polyubiquitination and degradation of SNC1 and RPS2. MUSE3 appears to function with SNC1 through direct protein–protein interaction, while its activity with RPS2 seems indirect (Supplemental Figure 8).

DISCUSSION

In eukaryotes, selective protein degradation by the Ub/proteasome system primarily requires E1, E2, and E3 enzymes. However, E4 activity is often needed for polyubiquitination of many target proteins to ensure efficient downstream degradation (Koegl et al., 1999; Hoppe, 2005). E4 factors often catalyze polyubiquitin chain assembly in conjunction with E1, E2, and E3 enzymes. The first and best-studied example of E4 function is UFD2, encoded by a single-copy gene in yeast. In the work of Koegl et al. (1999), UFD2 efficiently facilitates the polyubiquitination of Ub-ProtA, a model UFD substrate, only together with E1, E2, and E3 but not with just E1 and E2, suggesting the requirement of E3 for E4 function on certain substrates. Subsequent studies demonstrated that Ufd2p can also act as an E3 ligase, as it is able to bind to E2 and its U-box domain is structurally similar to the E3 RING domains (Tu et al., 2007). The two proposed possible working models of UFD2 and its corresponding E3 Ufd4p are (1) a sequential model, where UFD2 functions downstream of Ufd4p to add further Ubs to the substrate, and (2) a cooperative model, in which UFD2 works in conjunction with E3 Ufd4p for polyubiquitin chain assembly (Tu et al., 2007). Although UFD2 is an evolutionarily conserved protein present in all eukaryotes, it biological function in plants has never been studied.

(E) Bacterial growth of *Pseudomonas* (*P.s.m.*) ES4326 on wild-type, *muse3-1*, and *muse3-2* plants. Leaves of 4-week-old plants were infiltrated with a bacterial suspension at OD_{600} = 0.0005. Leaf discs within the infected area were taken right after infiltration (day 0) and 3 d after infiltration (day 3) to quantify bacterial colony-forming units (cfu). Bars represent means of five replicates ± SD. One-way ANOVA was used to calculate statistical significance between genotypes as indicated by different letters ($P < 0.0005$).

(F) SNC1 protein levels in the wild type, *muse3-1*, and *muse3-2*. Signals from nonspecific proteins (NSPs) served as internal loading controls.

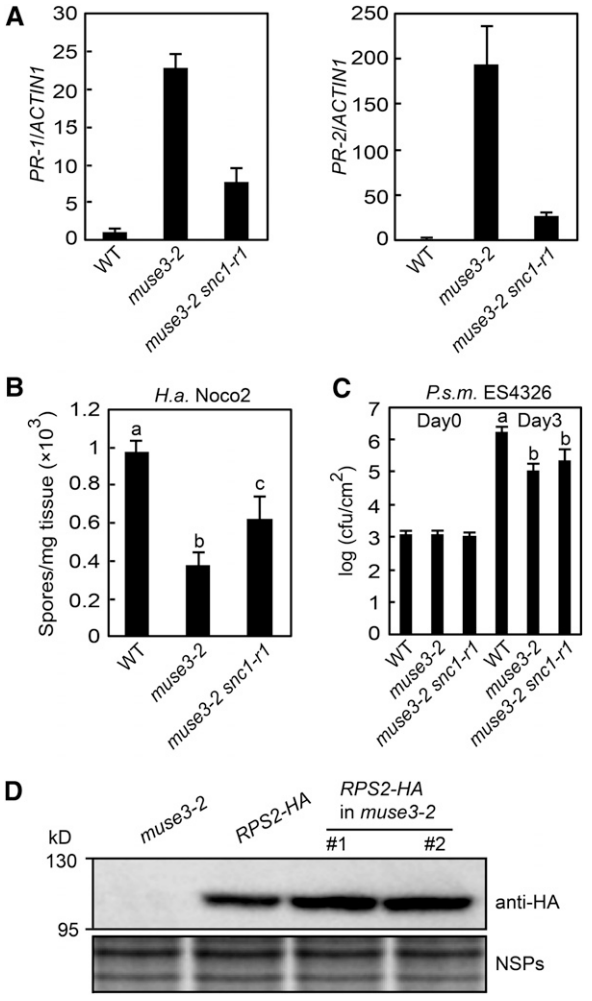

Figure 6. The Loss-of-Function *snc1-r1* Allele Partially Suppresses the Constitutive Defense Phenotypes of *muse3-2*.

(A) Relative expression of *PR-1* and *PR-2* in the wild type, *muse3-2*, and *muse3-2 snc1-r1* as determined by real-time RT-PCR. Total RNA was extracted from 3-week-old soil-grown plants and reverse transcribed to cDNA. The *PR-1*, *PR-2*, and *SNC1* transcript levels were normalized by *ACTIN1*. Data are mean values of three replicates ± SD. Three independent experiments were performed with similar results.

(B) Growth of *H. arabidopsidis* (*H.a.*) Noco2 sporulation on wild-type, *muse3-2*, and *muse3-2 snc1-r1* seedlings. One-way ANOVA was used to calculate statistical significance between genotypes as indicated by different letters ($P < 0.05$). Data are mean values of four replicates ± SD.

(C) Bacterial growth of *Pseudomonas* (*P.s.m.*) ES4326 on the wild type, *muse3-2*, and *muse3-2 snc1-r1*. One-way ANOVA was used to calculate statistical significance between genotypes as indicated by different letters ($P < 0.05$). Data are mean values of four replicates ± SD.

(D) Immunoblot analysis of RPS2-HA protein levels in *muse3-2*. The *RPS2-HA* transgene was crossed into *muse3-2*. Data from two independent lines were shown. Signals from nonspecific proteins (NSPs) served as internal loading controls.

From this investigation, the putative *Arabidopsis* E4 factor MUSE3 complemented the yeast *ufd2*Δ knockout strain phenotypes (Figure 4), suggesting that MUSE3 has E4 activity and is an ortholog of UFD2. Since *muse3* mutant plants exhibited enhanced disease resistance and elevated levels of NLR proteins, including SNC1 and RPS2 (Figures 5 and 6), MUSE3 seems to play negative roles in plant immunity and turnover control of NLR receptors. Since the enhanced resistance in *muse3* is only partly due to increased SNC1 accumulation (Figure 6), we speculate that MUSE3 probably has multiple NLR targets. Previously, it was shown that the F-box protein CPR1, a component of an SCF E3 complex, targets SNC1 and RPS2 for degradation (Cheng et al., 2011; Gou et al., 2012). However, overexpression of *MUSE3* in the *snc1* background did not suppress *snc1*-associated morphological phenotypes or affect SNC1 accumulation (Figures 7C and 7D), suggesting that MUSE3 alone is not sufficient to affect SNC1 level. Transient coexpression of *SNC1* with *MUSE3* in *N. benthamiana* also demonstrated that MUSE3 alone is not sufficient to affect SNC1 or RPS2 accumulation (Figures 7A and 7B). However, when expressed with CPR1, MUSE3 can enhance SNC1 and RPS2 degradation in *N. benthamiana* (Figures 7A and 7B). This is also true when both CPR1 and MUSE3 are stably transformed in *Arabidopsis* (Figure 7D). These biochemical data thus support the sequential model where MUSE3 seems to act downstream of CPR1 to facilitate SNC1 and RPS2 degradation (Supplemental Figure 8). It is likely that Ub is first transferred via the E3 SCF^{CPR1} complex to substrates including SNC1 and RPS2. After adding one to three Ub moieties, the SCF^{CPR1} E3 complex may become inactive and dissociate from the substrates. The ubiquitinated substrates may recruit MUSE3 and an E2 in order to transfer additional Ubs from the E2 to the substrates. The polyubiquitinated substrates thus become efficient substrates for proteasome degradation. This sequential model is further supported by our Co-IP data showing that MUSE3 associates with SNC1 but not with CPR1 (Figures 8A and 8C; Supplemental Figures 7A and 7C).

Although both SNC1 and RPS2 seem to be substrates of MUSE3, we believe that the modes of action of MUSE3 on these targets may be different. SNC1 appears to directly interact with MUSE3 (Figure 8; Supplemental Figure 7), whereas the MUSE3–RPS2 interaction may require an unknown adaptor or facilitator protein. Unlike with SNC1, for which polyubiquitinated forms of the protein were never observed on immunoblots, in half of our coexpression experiments with RPS2 in *N. benthamiana*, we were able to detect laddering signals that are presumed to represent a variety of polyubiquitinated forms of RPS2 (Supplemental Figure 5). The polyubiquitinated RPS2 signals appear to be slightly stronger when coexpressing *CPR1* and *MUSE3* compared with expressing *CPR1* alone (Supplemental Figure 5), suggesting that MUSE3 has E4 activity that is involved in efficient polyubiquitin chain assembly. We are not sure why laddering was not observed consistently in all experiments. It may be due to subtle differences in tissue collection and growth conditions. In addition, higher molecular weight signals above RPS2-FLAG were detected in the beads fraction of our Co-IP experiment, and these were confirmed to correspond to polyubiquitinated forms of RPS2 by immunoblotting with anti-Ub antibody (Figure 8B). The polyubiquitinated laddering pattern

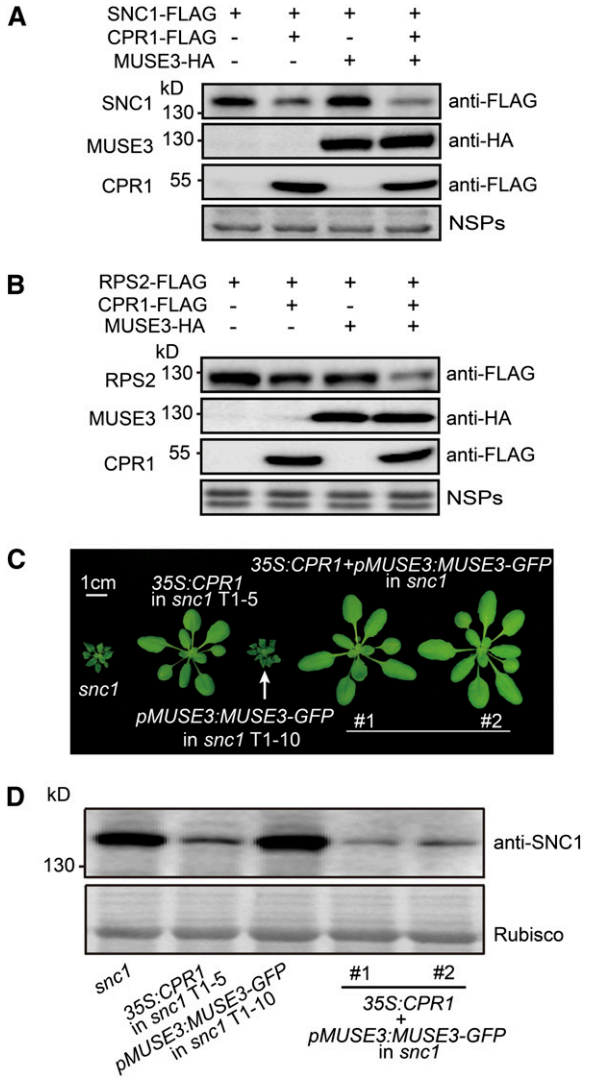

Figure 7. MUSE3 Facilitates CPR1-Mediated Degradation of SNC1 and RPS2.

(A) SNC1-FLAG, MUSE3-HA, and CPR1-FLAG levels in *N. benthamiana* leaves expressing the indicated proteins. Signals from nonspecific proteins (NSPs) served as internal loading controls.

(B) RPS2-FLAG, MUSE3-HA, and CPR1-FLAG levels in *N. benthamiana* leaves expressing the indicated proteins. Signals from nonspecific proteins (NSPs) served as internal loading controls.

(C) Morphology of 4-week-old soil-grown plants of the indicated genotypes. #1 and #2 are two independent F3 lines homozygous for *snc1*, *35S:CPR1*, or *pMUSE3:MUSE3-GFP* that were identified from a cross between *35S:CPR1* in *snc1* (T1-5; Cheng et al., 2011) and *pMUSE3:MUSE3-GFP* in *snc1* (T1-10). Bar = 1 cm.

(D) Immunoblot analysis of SNC1 protein levels in the indicated genotypes. Total protein was extracted from 4-week-old soil-grown plants. Rubisco levels served as the internal loading control.

was never observed for SNC1 samples, indicating that the turnover rate of polyubiquitinated RPS2 and SNC1 is probably different. Even with the application of the proteasome inhibitor MG132, we only observed higher SNC1 accumulation but never polyubiquitinated forms of the protein (Supplemental Figure 6), indicating that they may be too transient or unstable to be detected.

An important avenue of further investigation will be to identify other NLRs being targeted by MUSE3. We do not expect all R proteins to be targeted by MUSE3, since the enhanced immunity of *muse3* mutants is not severe (Figure 5). How MUSE3 achieves its substrate specificity will also be an interesting question to address in future studies.

We are likewise intrigued by the very mild growth defects observed in the *muse3* mutants. Although *MUSE3*/*UFD2* family genes are highly conserved in eukaryotes, the phenotypes of the mutants suggest that they are not needed for most other biological processes, including general plant growth and development under laboratory conditions. In yeast and humans, UFD2 was found to target many substrates involved in different processes; thus, it is unlikely that MUSE3 is solely dedicated to immune response regulation in the plant kingdom. In the *Arabidopsis* genome, there are two E1s, more than 37 E2s, and over

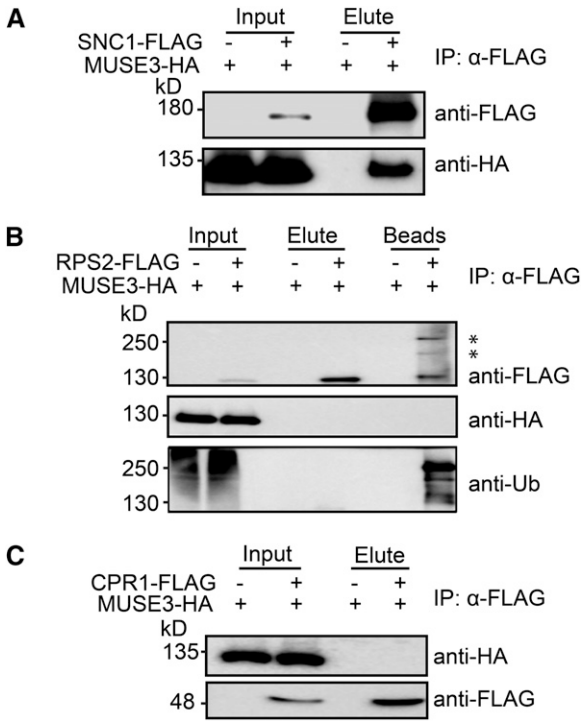

Figure 8. MUSE3 Directly Associates with SNC1 but Not with RPS2 and CPR1.

(A) In planta Co-IP of MUSE3-HA using SNC1-FLAG.

(B) In planta Co-IP of MUSE3-HA using RPS2-FLAG. The polyubiquitinated forms of RPS2 detected (indicated with asterisks) were confirmed when the same samples were probed with anti-Ub antibody in immunoblot analyses.

(C) In planta Co-IP of MUSE3-HA using CPR1-FLAG.

N. benthamiana leaves were infiltrated with *Agrobacterium* cells containing constructs expressing the indicated proteins. Total protein extracts were subjected to immunoprecipitation (IP) with anti-FLAG agarose beads. Input, Elute, and Beads fractions were probed with anti-FLAG or anti-HA antibodies in immunoblot analyses.

1300 potential E3s (Hatfield et al., 1997; Bachmair et al., 2001; Vierstra, 2003). As the most numerous and diverse components of ubiquitination pathways, these E3s determine the specificity of substrates in various biological processes (Smalle and Vierstra, 2004; Liu et al., 2012). MUSE3, as the only E4 identified in *Arabidopsis*, most likely helps a variety of E3 ligases for efficient degradation of their substrates. Therefore, it will be important in the future to perform a variety of detailed phenotypic analyses of *muse3* mutants in the plant research community in order to reveal other important E3 partners and protein targets of MUSE3 in additional biological processes other than immunity.

METHODS

Plant Growth Conditions and Mutant Screen

All *Arabidopsis thaliana* plants were grown in climate-controlled chambers at 22°C under a 16-h-light (120 μmol m^{-2} s^{-1})/8-h-dark cycle. The *muse* screen using ethyl methanesulfonate was performed as described previously (Huang et al., 2013). *muse3-1* was identified from the screen in the *mos4-1 snc1* background. The primers for mutant genotyping are as follows: *mos4*-F, 5′-CTGGCTTTTGGAACTTAACCAC-3′, and *mos4*-R, 5′-GATCTGTGTCTCAAGCATGGC-3′; *snc1_Xba*I-NF, 5′-ATGAGGTGGAGTTCCCATCTG-3′, and *snc1_Xba*I-NR, 5′-CATCCCATTTTGATTGCTGGAAAG-3′; *MUSE3*_WT-F, 5′-AACAAGACTCTTCCATTCGC-3′, *MUSE3*_Mutant-F, 5′-AACAAGACTCTTCCATTgGt-3′, and *MUSE3*_R, 5′-TAGTCACATCTTCATTTGCC-3′; SAIL_713_A12 (*muse3-2*)-LP, 5′-AGATGGCACCAGGGAATATG-3′, and SAIL_713_A12 (*muse3-2*)-RP, 5′-GTGAGCTTGCCATGACTTTG-3′.

Gene Expression Analysis

About 70 mg of total plant tissue was collected from 2-week-old seedlings grown on half-strength Murashige and Skoog (MS) medium. RNA was extracted using the Totally RNA kit (Ambion, now part of Invitrogen). Superscript II reverse transcriptase (Invitrogen) was used to reverse transcribe 0.4 μg of total RNA to obtain cDNA. Levels of cDNAs were initially normalized with *ACTIN1* by real-time PCR using the QuantiFAST SYBR Green PCR kit (Qiagen). For RT-PCR, the cDNA was amplified by PCR using 94°C for 2 min and 28 cycles of 94°C for 20 s, 58°C for 30 s, and 68°C for 1 min. The products were subsequently analyzed by agarose gel electrophoresis and ethidium bromide staining. *ACTIN1* expression was used to standardize transcript levels in each sample. The primers for RT-PCR analyses used in this study are as follows: *PR-1*-F, 5′-GTAGGTGCTCTTGTTCTTCCC-3′, and *PR-1*-R, 5′-CACATAATTCCCACGAGGATC-3′; *PR-2*-F, 5′-GCTTCCTTCTTCAACCACACAGC-3′, and *PR-2*-R, 5′-CGTTGATGTACCGGAATCTGAC-3′; *ACTIN1*-F, 5′-CGATGAAGCTCAATCCAAACGA-3′, and *ACTIN1*-R, 5′-CAGAGTCGAGCACAATACCG-3′; *SNC1*-F, 5′-AGATGTCCCCGATGTCATCC-3′, and *SNC1*-R, 5′-CCAAACATTTTCAGACTTACAAGACTTG-3′.

Pathogen Infections

Infection experiments with the oomycete *Hyaloperonospora arabidopsidis* Noco2 and *Pseudomonas syringae* pv *maculicola* ES4326 were performed as described (Li et al., 2001). Briefly, *H. arabidopsidis* Noco2 infection was performed on 2-week-old seedlings by spraying *H. arabidopsidis* Noco2 spore suspension at the concentrations indicated in the figure legends. Plants were maintained at 18°C under a 12-h-light/12-h-dark cycle with 80% humidity, and the infection level was quantified 7 d after inoculation by counting the number of conidiospores per gram of tissue using a hemocytometer.

Total Protein Extraction

Fifty milligrams of leaf tissue from 4-week-old soil-grown plants was harvested and ground into powder using liquid nitrogen. The samples were homogenized in extraction buffer (100 mM Tris-HCl, pH 8, 0.1% SDS, and 2% β-mercaptoethanol). After centrifuging for 5 min at 13,200 rpm in a standard microfuge, the supernatant of each sample was transferred to a new microtube with 4× Laemmli loading buffer (60 mM Tris-Cl, pH 6.8, 2% SDS, 10% glycerol, 5% β-mercaptoethanol, and 0.01% bromophenol blue) and boiled for 5 min at 95°C. The sample was diluted to a final concentration of 1× loading buffer. Immunoblot analysis was performed afterward to analyze samples using specific antibodies. The anti-FLAG antibody and anti-Ub antibodies were from Sigma-Aldrich. The anti-HA antibody was from Roche.

Positional Cloning and Illumina Whole-Genome Sequencing

Positional cloning of *muse3-1* was performed using a previously described strategy (Huang et al., 2013). The markers used for mapping were designed according to the insertion/deletion or single nucleotide polymorphisms between the genomic sequences of Columbia and Landsberg *erecta* ecotypes that are available on TAIR (http://www.Arabidopsis.org). Once the site of the mutation was localized to a small region of ~1 Mb, the genomic DNAs of mutant seedlings from the mapping population were sequenced with Illumina whole-genome sequencing following the instruction manual from New England Biolabs. Briefly, the purified genomic DNA was sonicated into fragments of ~300 bp, which were set to end repair, dA tailing, and adaptor ligation. After removal of unligated adapters, the ligated DNA was enriched by PCR to create a genomic DNA library. The genomic DNA library was then sequenced using an Illumina genome analyzer. After comparison with wild-type genomic sequence, the potential mutations within the flanking area were further analyzed by Sanger sequencing.

Construction of Plasmids

The *MUSE3* genomic sequence plus 1.5-kb regions both upstream of the start codon and downstream of the stop codon was amplified by primers 5′-CGCGGATCCGAAGATCTTAGGTACATTACCG-3′ and 5′-ACGCGTCGACTTACGATATGGACTGGTCATGC-3′ from wild-type genomic DNA. The amplified fragment was then digested with *Bam*HI and *Sal*I and cloned into the modified *pCAMBIA1305-GFP* to generate *pCAMBIA1305-pMUSE3:MUSE3*. For the construction of *pCAMBIA1305-pMUSE3:MUSE3-GFP*, the fragment containing 1.5-kb sequence upstream of the start codon of *MUSE3* and the *MUSE3* genomic sequence without the stop codon was amplified by 5′-CGCGGATCCGAAGATCTTAGGTACATTACCG-3′ and 5′-GTCGACATCAATTAACATAT-3′. After *Bam*HI and *Sal*I digestion, the fragment was ligated into *pCAMBIA1305-GFP*. These constructs were electroporated into *Agrobacterium tumefaciens* strain GV3101 and subsequently transformed into *muse3-1 mos4 snc1* by a floral dipping method (Clough and Bent, 1998). For transient expression experiments in *Nicotiana benthamiana*, the coding sequence of *MUSE3* was PCR amplified from wild-type cDNA using primers 5′-CGGGGTACCATGGCGACGAGCAAACCTCA-3′ and 5′-CGCGGATCCATCAATTAACATATCACTGTTTGTAG-3′. The amplified fragment was then digested with *Kpn*I and *Bam*HI and cloned into *pCAMBIA1300-35S-3×HA* to generate *pCAMBIA1300-35S:MUSE3-3×HA*. The plasmid was electroporated into *Agrobacterium* and used for transient expression and Co-IP in *N. benthamiana*. For yeast complementation, full-length *MUSE3* cDNA was PCR cloned into yeast expression vector p425-GPD with primers 5′-CGCGGATCCATGGCGACGAGCAAACCTCA-3′ and 5′-ACGCGTCGACTTAATCAATTAACATATCACTGTTTGTAG-3′, using *Bam*HI and *Sal*I digestion sites for inserting *MUSE3* behind the GPD promoter. The yeast *ufd2*Δ mutant strain was obtained from the yeast deletion collection (Open Biosystems). MUSE3 and

empty vector control plasmids were introduced into *ufd2*Δ and wild-type yeast strains using a standard polyethylene glycol/lithium acetate yeast transformation protocol (http://labs.fhcrc.org/gottschling/Yeast%20Protocols/ytrans.html). Yeast transformants were grown overnight, serially diluted, and plated onto the appropriate media to assay for growth.

Subcellular Fractionation

Subcellular fractionation of MUSE3-GFP was performed as described previously (Cheng et al., 2009). In brief, 2-week-old plate-grown seedlings (1 g) were harvested and ground to a fine powder in liquid nitrogen and mixed with 2 mL of cold lysis buffer (20 mM Tris-HCl, pH 7.4, 25% glycerol, 20 mM KCl, 2 mM EDTA, 2.5 mM $MgCl_2$, 250 mM Suc, and 1 mM phenylmethylsulfonyl fluoride). The homogenate was filtered through 95- and 40-μm nylon mesh sequentially. The flow-through was spun at 1500*g* for 10 min, and the supernatant consisting of the cytosolic fraction was collected and mixed with 4× Laemmli loading buffer and heated at 95°C for 5 min. The pellet was washed four times with 3 mL of nuclear resuspension buffer consisting of 20 mM Tris-HCl, pH 7.4, 25% glycerol, 2.5 mM $MgCl_2$, and 0.2% Triton X-100. The final pellet was mixed with 50 μL of 1× Laemmli loading buffer and heated at 95°C for 5 min. Then, two fractions were loaded on a 10% SDS-PAGE gel for protein separation. Antibodies used for immunoblot analyses were as described: anti-histone H3 (Feys et al., 2005), anti-GFP (Wirthmueller et al., 2007), and anti-PEPC (Noël et al., 2007)

Transient Expression and Co-IP in *N. benthamiana*

Transient expression in *N. benthamiana* was performed as described previously (Van den Ackerveken et al., 1996). The Co-IP experiment was performed following the protocol from Moffett et al. (2002), with minor modifications. *Agrobacterium* strains expressing the target genes with specific tags under the control of the 35S promoter were first inoculated in Luria-Bertani medium with kanamycin selection and grown at 28°C for 16 to 18 h. Then, the bacterial cells were transferred into the new culture medium [10.5 g/L K_2HPO_4, 4.5 g/L KH_2PO_4, 1.0 g/L $(NH_4)_2SO_4$, 0.5 g/L sodium citrate, 1 mM $MgSO_4$, 0.2% Glc, 0.5% glycerol, 50 μM acetosyringone, 10 mM MES, pH 5.6, and 50 μg/mL kanamycin] by 1:50 dilution and incubated for 8 to 12 h. The bacteria were then pelleted at 3000*g* for 10 min and resuspended in MS buffer (4.4 g/L MS medium, 10 mM MES, and 150 μM acetosyringone), and two strains were mixed to a final concentration of OD_{600} = 0.3 for infiltration on 4-week-old *N. benthamiana* leaves.

For protein immunoprecipitation, ~4 g of *N. benthamiana* leaf tissue was harvested 38 h after infiltration and ground to a fine powder in liquid nitrogen. Two milliliters of extraction buffer per 1 g of tissue (10% glycerol, 25 mM Tris, pH 7.5, 1 mM EDTA, 150 mM NaCl, 10 mM DTT, 2% [w/v] polyvinylpolypyrrolidone, and 1% protease inhibitor cocktail [Roche]) was added to the powder and homogenized by further grinding. The sample was spun at 15,000*g* for 10 min at 4°C. Ninety microliters of the supernatant was saved as input. Thirty microliters of prewashed protein A or protein G beads was subsequently added to the rest of the supernatant containing 0.15% Nonidet P-40 (Nonidet P-40 substitute). After 30 min of incubation at 4°C, the mixture was spun at 3000*g* for 1 min to remove the beads. The supernatant was transferred to a tube with 30 μL of anti-FLAG M2 beads (Sigma-Aldrich) and incubated with agitation for 3 h at 4°C. The beads were then spun down at 8000 rpm in a microfuge for 1 min at 4°C and washed eight times with 1 mL of extraction buffer containing 0.15% Nonidet P-40 before immunoprecipitated proteins were eluted with 100 μL of 250 μg/mL 3× FLAG peptides (Sigma-Aldrich). SDS loading buffer was added to each sample and boiled for 5 min. The samples were run on SDS-PAGE gels for further immunoblot analysis.

Accession Numbers

Sequence data from this article can be found in the GenBank/EMBL database or the Arabidopsis Genome Initiative database under the following accession numbers: *At5g15400*, NP_568313 (*MUSE3*); *At4g16890*, NP_193422 (*SNC1*); *At3g18165*, NP_566599 (*MOS4*); *At2g14610*, NP_179068 (*PR-1*); *At3g57260*, NP_191285 (*PR-2*); *At2g37620*, NP_566988 (*ACTIN1*). The accession numbers for all the sequences used in phylogenetic analysis include the following: XP_002873722 (*Arabidopsis lyrata*); NP_010091 (*Saccharomyces cerevisiae UFD2*); NP_004779 (*Homo sapiens UBE4A*); NP_006039 (*H. sapiens UBE4B*); XP_001777615 (*Physcomitrella patens*); XP_002532897 (*Ricinus communis*); XP_002324089 (*Populus trichocarpa*); XP_003633847 (*Vitis vinfera*); BAK06841 (*Hordeum vulgare*); EAZ27404 (*Oryza sativa japonica*); EAY90539 (*Oryza sativa indica*); XP_002467679 (*Sorghum bicolor*); XP_002964116 (*Selaginella moellendorffii*); XP_001422027 (*Ostreococcus lucimarinus*); XP_003064107 (*Micromonas pusilla*); NP_071305 (*Mus musculus*). The T-DNA insertion allele of *muse3* (renamed *muse3-2*) is designated SAIL_713_A12.

Supplemental Data

The following materials are available in the online version of this article.

Supplemental Figure 1. Phylogenetic Relationship between MUSE3 and Its Homologs.

Supplemental Figure 2. Multiple Alignments of MUSE3, Yeast UFD2, and Human UBE4.

Supplemental Figure 3. *MUSE3* Complements the Molecular Lesion in *muse3-1 mos4 snc1*.

Supplemental Figure 4. *MUSE3-GFP* Localizes to Both Nuclei and Cytoplasm.

Supplemental Figure 5. MUSE3 Facilitates CPR1-Mediated Degradation of RPS2.

Supplemental Figure 6. MG132 Treatment Enhances SNC1 Accumulation, although No Polyubiquitinated Form of SNC1 Was Detected.

Supplemental Figure 7. MUSE3 Associates with SNC1 but Not with RPS2 and CPR1 Directly.

Supplemental Figure 8. A Sequential Model of How MUSE3 Facilitates CPR1-Mediated SNC1 and RPS2 Degradation.

Supplemental Data Set 1. Text File of the Sequences and Alignment Used for the Phylogenetic Analysis Shown in Supplemental Figure 1.

Supplemental References.

ACKNOWLEDGMENTS

We thank Yan Li and Yuelin Zhang (University of British Columbia and NIBS, China) for Illumina sequencing of *muse3-1* and mutation analysis, Kaeli Johnson for critical reading of the manuscript, and Brian Staskawitz (University of California, Berkeley) for seeds of the *RPS2-HA* transgenic line. This article was supported by the Natural Sciences and Engineering Research Council of Canada (to X.L.), by the Chinese Scholarship Council (Ph.D. scholarship to Y.H.), and by the Deutsche Forschungsgemeinschaft (to C.R., V.L., and M.W.).

AUTHOR CONTRIBUTIONS

Y.H. performed most of the experiments under the supervision of X.L. The confocal images of MUSE3-GFP were produced by C.R., V.L., and M.W. The yeast *ufd2* knockout strain for the yeast complementation test was generated by S.M. S.H. carried out the phylogenetic analysis. Y.H.

and X.L. wrote the manuscript. All authors contributed to the revision of the manuscript.

Received September 24, 2013; revised December 12, 2013; accepted January 8, 2014; published January 21, 2014.

REFERENCES

Aarts, N., Metz, M., Holub, E., Staskawicz, B.J., Daniels, M.J., and Parker, J.E. (1998). Different requirements for EDS1 and NDR1 by disease resistance genes define at least two R gene-mediated signaling pathways in Arabidopsis. Proc. Natl. Acad. Sci. USA **95:** 10306–10311.

Axtell, M.J., and Staskawicz, B.J. (2003). Initiation of RPS2-specified disease resistance in Arabidopsis is coupled to the AvrRpt2-directed elimination of RIN4. Cell **112:** 369–377.

Bachmair, A., Novatchkova, M., Potuschak, T., and Eisenhaber, F. (2001). Ubiquitylation in plants: A post-genomic look at a post-translational modification. Trends Plant Sci. **6:** 463–470.

Bent, A.F., and Mackey, D. (2007). Elicitors, effectors, and R genes: The new paradigm and a lifetime supply of questions. Annu. Rev. Phytopathol. **45:** 399–436.

Cheng, Y.T., and Li, X. (2012). Ubiquitination in NB-LRR-mediated immunity. Curr. Opin. Plant Biol. **15:** 392–399.

Cheng, Y.T., Li, Y., Huang, S., Huang, Y., Dong, X., Zhang, Y., and Li, X. (2011). Stability of plant immune-receptor resistance proteins is controlled by SKP1-CULLIN1-F-box (SCF)-mediated protein degradation. Proc. Natl. Acad. Sci. USA **108:** 14694–14699.

Cheng, Y.T., Germain, H., Wiermer, M., Bi, D., Xu, F., García, A.V., Wirthmueller, L., Després, C., Parker, J.E., Zhang, Y., and Li, X. (2009). Nuclear pore complex component MOS7/Nup88 is required for innate immunity and nuclear accumulation of defense regulators in *Arabidopsis*. Plant Cell **21:** 2503–2516.

Clough, S.J., and Bent, A.F. (1998). Floral dip: A simplified method for Agrobacterium-mediated transformation of *Arabidopsis thaliana*. Plant J. **16:** 735–743.

Feys, B.J., Wiermer, M., Bhat, R.A., Moisan, L.J., Medina-Escobar, N., Neu, C., Cabral, A., and Parker, J.E. (2005). *Arabidopsis* SENESCENCE-ASSOCIATED GENE101 stabilizes and signals within an ENHANCED DISEASE SUSCEPTIBILITY1 complex in plant innate immunity. Plant Cell **17:** 2601–2613.

Gou, M., Shi, Z., Zhu, Y., Bao, Z., Wang, G., and Hua, J. (2012). The F-box protein CPR1/CPR30 negatively regulates R protein SNC1 accumulation. Plant J. **69:** 411–420.

Hatfield, P.M., Gosink, M.M., Carpenter, T.B., and Vierstra, R.D. (1997). The ubiquitin-activating enzyme (E1) gene family in *Arabidopsis thaliana*. Plant J. **11:** 213–226.

Hershko, A., and Ciechanover, A. (1998). The ubiquitin system. Annu. Rev. Biochem. **67:** 425–479.

Hochstrasser, M. (1996). Ubiquitin-dependent protein degradation. Annu. Rev. Genet. **30:** 405–439.

Hoppe, T. (2005). Multiubiquitylation by E4 enzymes: 'One size' doesn't fit all. Trends Biochem. Sci. **30:** 183–187.

Hoppe, T., Cassata, G., Barral, J.M., Springer, W., Hutagalung, A.H., Epstein, H.F., and Baumeister, R. (2004). Regulation of the myosin-directed chaperone UNC-45 by a novel E3/E4-multiubiquitylation complex in *C. elegans*. Cell **118:** 337–349.

Huang, Y., Chen, X., Liu, Y., Roth, C., Copeland, C., McFarlane, H.E., Huang, S., Lipka, V., Wiermer, M., and Li, X. (2013). Mitochondrial AtPAM16 is required for plant survival and the negative regulation of plant immunity. Nat Commun **4:** 2558.

Johnson, E.S., Ma, P.C., Ota, I.M., and Varshavsky, A. (1995). A proteolytic pathway that recognizes ubiquitin as a degradation signal. J. Biol. Chem. **270:** 17442–17456.

Jones, J.D., and Dangl, J.L. (2006). The plant immune system. Nature **444:** 323–329.

Koegl, M., Hoppe, T., Schlenker, S., Ulrich, H.D., Mayer, T.U., and Jentsch, S. (1999). A novel ubiquitination factor, E4, is involved in multiubiquitin chain assembly. Cell **96:** 635–644.

Li, X., Clarke, J.D., Zhang, Y., and Dong, X. (2001). Activation of an EDS1-mediated R-gene pathway in the snc1 mutant leads to constitutive, NPR1-independent pathogen resistance. Mol. Plant Microbe Interact. **14:** 1131–1139.

Li, Y., Li, S., Bi, D., Cheng, Y.T., Li, X., and Zhang, Y. (2010). SRFR1 negatively regulates plant NB-LRR resistance protein accumulation to prevent autoimmunity. PLoS Pathog. **6:** e1001111.

Liu, J., Li, W., Ning, Y., Shirsekar, G., Cai, Y., Wang, X., Dai, L., Wang, Z., Liu, W., and Wang, G.L. (2012). The U-box E3 ligase SPL11/PUB13 is a convergence point of defense and flowering signaling in plants. Plant Physiol. **160:** 28–37.

Liu, Y., Schiff, M., Serino, G., Deng, X.W., and Dinesh-Kumar, S.P. (2002). Role of SCF ubiquitin-ligase and the COP9 signalosome in the N gene-mediated resistance response to *Tobacco mosaic virus*. Plant Cell **14:** 1483–1496.

Maekawa, T., Kufer, T.A., and Schulze-Lefert, P. (2011). NLR functions in plant and animal immune systems: So far and yet so close. Nat. Immunol. **12:** 817–826.

Matsumoto, M., Yada, M., Hatakeyama, S., Ishimoto, H., Tanimura, T., Tsuji, S., Kakizuka, A., Kitagawa, M., and Nakayama, K.I. (2004). Molecular clearance of ataxin-3 is regulated by a mammalian E4. EMBO J. **23:** 659–669.

Moffett, P., Farnham, G., Peart, J., and Baulcombe, D.C. (2002). Interaction between domains of a plant NBS-LRR protein in disease resistance-related cell death. EMBO J. **21:** 4511–4519.

Noël, L.D., Cagna, G., Stuttmann, J., Wirthmüller, L., Betsuyaku, S., Witte, C.P., Bhat, R., Pochon, N., Colby, T., and Parker, J.E. (2007). Interaction between SGT1 and cytosolic/nuclear HSC70 chaperones regulates *Arabidopsis* immune responses. Plant Cell **19:** 4061–4076.

Palma, K., Zhao, Q., Cheng, Y.T., Bi, D., Monaghan, J., Cheng, W., Zhang, Y., and Li, X. (2007). Regulation of plant innate immunity by three proteins in a complex conserved across the plant and animal kingdoms. Genes Dev. **21:** 1484–1493.

Pickart, C.M. (2001). Mechanisms underlying ubiquitination. Annu. Rev. Biochem. **70:** 503–533.

Pukatzki, S., Tordilla, N., Franke, J., and Kessin, R.H. (1998). A novel component involved in ubiquitination is required for development of *Dictyostelium discoideum*. J. Biol. Chem. **273:** 24131–24138.

Shirano, Y., Kachroo, P., Shah, J., and Klessig, D.F. (2002). A gain-of-function mutation in an *Arabidopsis* Toll Interleukin1 receptor-nucleotide binding site-leucine-rich repeat type R gene triggers defense responses and results in enhanced disease resistance. Plant Cell **14:** 3149–3162.

Shirasu, K. (2009). The HSP90-SGT1 chaperone complex for NLR immune sensors. Annu. Rev. Plant Biol. **60:** 139–164.

Smalle, J., and Vierstra, R.D. (2004). The ubiquitin 26S proteasome proteolytic pathway. Annu. Rev. Plant Biol. **55:** 555–590.

Staskawicz, B.J., Ausubel, F.M., Baker, B.J., Ellis, J.G., and Jones, J.D. (1995). Molecular genetics of plant disease resistance. Science **268:** 661–667.

Trujillo, M., and Shirasu, K. (2010). Ubiquitination in plant immunity. Curr. Opin. Plant Biol. **13:** 402–408.

Tu, D., Li, W., Ye, Y., and Brunger, A.T. (2007). Structure and function of the yeast U-box-containing ubiquitin ligase Ufd2p. Proc. Natl. Acad. Sci. USA **104:** 15599–15606.

Van den Ackerveken, G., Marois, E., and Bonas, U. (1996). Recognition of the bacterial avirulence protein AvrBs3 occurs inside the host plant cell. Cell **87:** 1307–1316.

Vierstra, R.D. (2003). The ubiquitin/26S proteasome pathway, the complex last chapter in the life of many plant proteins. Trends Plant Sci. **8:** 135–142.

Wirthmueller, L., Zhang, Y., Jones, J.D., and Parker, J.E. (2007). Nuclear accumulation of the Arabidopsis immune receptor RPS4 is necessary for triggering EDS1-dependent defense. Curr. Biol. **17:** 2023–2029.

Zeng, L.R., Qu, S., Bordeos, A., Yang, C., Baraoidan, M., Yan, H., Xie, Q., Nahm, B.H., Leung, H., and Wang, G.L. (2004). Spotted leaf11, a negative regulator of plant cell death and defense, encodes a U-box/armadillo repeat protein endowed with E3 ubiquitin ligase activity. Plant Cell **16:** 2795–2808.

Zhang, Y., Goritschnig, S., Dong, X., and Li, X. (2003). A gain-of-function mutation in a plant disease resistance gene leads to constitutive activation of downstream signal transduction pathways in suppressor of npr1-1, constitutive 1. Plant Cell **15:** 2636–2646.